



1 **Monthly trends of methane emissions in Los Angeles from 2011**  
2 **to 2015 inferred by CLARS-FTS observations**

3

4 Kam W. Wong<sup>1,2</sup>, Thomas J. Pongetti<sup>1</sup>, Tom Oda<sup>3,4</sup>, Preeti Rao<sup>1</sup>, Kevin. R. Gurney<sup>5</sup>, Sally  
5 Newman<sup>2</sup>, Riley M. Duren<sup>1</sup>, Charles E. Miller<sup>1</sup>, Yuk L. Yung<sup>2</sup> and Stanley P. Sander<sup>1</sup>

6

7 <sup>1</sup>NASA Jet Propulsion Laboratory, California Institute of Technology, Pasadena, California,  
8 USA

9 <sup>2</sup>Division of Geological and Planetary Sciences, California Institute of Technology, Pasadena,  
10 California, USA

11 <sup>3</sup>Goddard Earth Sciences Technology and Research, Universities Space Research Association,  
12 Columbia, Maryland, USA

13 <sup>4</sup>Global Modeling and Assimilation Office, NASA Goddard Space Flight Center, Greenbelt,  
14 Maryland, USA

15 <sup>5</sup>School of Life Sciences, Arizona State University, Tempe, Arizona, USA

16 *Correspondence to:* K. W. Wong (clare.wong@jpl.nasa.gov)

17

18 © 2016. All rights reserved.

19



1 **Abstract.** This paper presents an analysis of methane emissions from the Los Angeles basin at  
2 monthly timescales across a four-year time period – from September 2011 to August 2015.  
3 Using observations acquired by a ground-based near-infrared remote sensing instrument on  
4 Mount Wilson, California combined with atmospheric CH<sub>4</sub>-CO<sub>2</sub> tracer-tracer correlations, we  
5 observed -18% to +22% monthly variability in CH<sub>4</sub>:CO<sub>2</sub> from the annual mean in the Los  
6 Angeles basin. Top-down estimates of methane emissions for the basin also exhibit significant  
7 monthly variability (-19% to +31% from annual mean and a maximum month-to-month change  
8 of 47%). During this period, methane emissions consistently peaked in the late summer/early fall  
9 and winter. The estimated annual methane emissions did not show a statistically significant trend  
10 over the 2011 to 2015 time period.  
11



## 1 **1 Introduction**

2 Methane (CH<sub>4</sub>) is a potent and newly regulated greenhouse gas in California. However, its  
3 emissions are poorly understood. In the South Coast Air Basin, which holds more than 43% of  
4 state's population, the annual methane emissions estimates based on atmospheric CH<sub>4</sub>  
5 observations indicate that the bottom-up emission inventory was systematically underestimated  
6 by 30% to >100% (Wong et al., 2015; Jeong et al., 2013; Peischl et al., 2013; Wennberg et al.,  
7 2012; Wunch et al., 2009; Wecht et al., 2014; Cui et al., 2015). Methane sources in the basin can  
8 be classified into two categories – biogenic and thermogenic. Biogenic methane is emitted from  
9 anaerobic digestion of organic matter by bacteria in waste management facilities, and by cattle in  
10 dairy farms. Waste management facilities include landfills, wastewater treatment plants and  
11 manure management facilities in dairy farms. Thermogenic methane emissions include natural  
12 sources, such as seeps and tar pits, and anthropogenic sources such as natural gas system leakage  
13 and gas/oil fields. Emissions from these sources are likely to have different seasonal patterns.  
14 Quantifying and tracking the seasonal variability will help us understand methane emissions and  
15 are essential for verifying emissions regulation and mitigation policies. However, most studies to  
16 date have been based on data from short-term measurement campaigns and have provided  
17 limited information on the temporal variability or trends of methane emissions in the basin  
18 (Peischl et al., 2013; Wecht et al., 2014; Cui et al., 2015; Wunch et al., 2009).

19 One commonly used approach to estimate CH<sub>4</sub> emissions from atmospheric observations is the  
20 tracer-tracer correlation technique. This method uses the regression slopes between observed  
21 trace gas mixing ratios (e.g. CH<sub>4</sub>:CO<sub>2</sub> or CH<sub>4</sub>:CO) in the atmosphere to calculate CH<sub>4</sub> emissions  
22 based on the more accurately known emissions of the correlate (e.g. CO<sub>2</sub> or CO). This method  
23 permits the derivation of the relative emissions of the two trace gases without the use of transport  
24 models and does not require the sources to be co-located (Wong et al., 2015; Peischl et al., 2013;  
25 Wennberg et al., 2012; Hsu et al., 2010; Wunch et al., 2009). Based on in situ flask observations  
26 on Mount Wilson, Hsu et al. (2010) did not observe any seasonal variability in the CH<sub>4</sub>:CO ratio  
27 from April 2007 to February 2008. Using column observations from the Total Carbon Column  
28 Observing Network (TCCON) in Pasadena, Wennberg et al. (2012) observed a ±15% monthly  
29 variability in the CH<sub>4</sub>:CO ratio between August 2007 to June 2008, but the monthly variability in  
30 methane emissions was not reported.



1 This paper presents the first study to quantify total methane emissions from an urban region at  
2 the monthly intervals and for an extended period of four years – from September 2011 to August  
3 2015. Using a unique dataset of mountaintop remote sensing observations acquired with the  
4 California Laboratory of Atmospheric Remote Sensing Fourier transform spectrometer (CLARS-  
5 FTS) (Wong et al., 2015; Fu et al., 2014), we have constructed a series of monthly CH<sub>4</sub>:CO<sub>2</sub>  
6 tracer-tracer correlations to, address the following questions:

- 7 1. What is the monthly variability in methane emissions in the Los Angeles basin?
- 8 2. Is there a detectable year-to-year methane emissions change in the basin?
- 9 3. What methane source(s) is(are) responsible for any observed temporal trends?

10

## 11 2 Methods

12 Since September 2011, continuous daytime ground-based remote sensing measurements of CH<sub>4</sub>  
13 and CO<sub>2</sub> have been acquired by a JPL-built Fourier transform spectrometer on Mount Wilson  
14 (Wong et al., 2015; Fu et al., 2014). The California Laboratory of Atmospheric Remote Sensing  
15 (CLARS) is located at an altitude of 1670 m above sea level with a panorama of the Los Angeles  
16 basin (Fig. 1). CLARS-FTS quantifies atmospheric column CH<sub>4</sub> and CO<sub>2</sub> using reflected sunlight  
17 in the near-infrared region. It operates in two measurement modes: Spectralon Viewing  
18 Observations (SVO) and Los Angeles Basin Surveys (LABS). In the SVO mode, the instrument  
19 quantifies the background tropospheric column CH<sub>4</sub> and CO<sub>2</sub> above the Los Angeles basin by  
20 measuring reflectance from a Spectralon® plate located at the CLARS site. In the LABS mode,  
21 the instrument samples the basin slant column CH<sub>4</sub> and CO<sub>2</sub> by measuring the surface reflection  
22 from 28 geographical locations (or reflection points) in the basin (Fig. 1). In each measurement  
23 cycle, we collect one set of LABS measurements and four SVO measurements. There are 5 to 8  
24 measurement cycles per day, depending on the time of the year.

25 Based on the Beer-Lambert Law, the slant column density (SCD) – the total number of absorbing  
26 molecule per unit area along the sun-Earth-instrument optical path – is retrieved for CH<sub>4</sub> at 1.67  
27 μm, CO<sub>2</sub> at 1.60 μm, and O<sub>2</sub> at 1.27 μm using a modified version of the GFIT algorithm  
28 developed at JPL (Fu et al., 2014; Wunch et al., 2011). The retrieved SCDs of CH<sub>4</sub> and CO<sub>2</sub> are  
29 then converted to slant column-averaged dry air mixing ratio, XCH<sub>4</sub> and XCO<sub>2</sub>, by normalizing



1 to the retrieved SCD of O<sub>2</sub> (SCD<sub>O<sub>2</sub></sub>) (Eq. 1).

$$2 \quad XGHG = \frac{SCD_{GHG}}{SCD_{O_2}} \times 0.2095 \quad (1)$$

3 Individual retrievals are analyzed with multiple post-processing filters to ensure data quality.  
 4 Spectra are removed when the residual root mean square errors of the fits to the GFIT radiative  
 5 transfer model exceed a pre-defined threshold. These are usually associated with aerosols, high  
 6 and low clouds, electrical or mechanical noise, and other transient behavior. Details about the  
 7 CLARS-FTS design, data retrieval algorithm and data filtering process are described in Fu et al.  
 8 (2014) and Wong et al. (2015).

9 Wong et al. (2015) mapped the spatial distribution of the CH<sub>4</sub>:CO<sub>2</sub> ratio and derived an annual  
 10 total CH<sub>4</sub> emission for the basin, based on CLARS-FTS observations from 2011 to 2013. Here  
 11 we used the same approach but focused on the temporal trend and quantify the monthly total CH<sub>4</sub>  
 12 emissions for the basin. Therefore, following Wong et al. (2015), we calculated the excess XCH<sub>4</sub>  
 13 and XCO<sub>2</sub>, due to the emissions from the basin, by subtracting the corresponding SVO  
 14 measurements from the LABS observations (Eq. 2).

$$15 \quad XGHG_{XS} = XGHG_{LABS} - XGHG_{SVO} \quad (2)$$

16 We then performed orthogonal distance regression (ODR) analyses of XCH<sub>4(XS)</sub> and XCO<sub>2(XS)</sub> for  
 17 the 28 reflection points for each month starting from September 2011 to August 2015. To  
 18 explore the overall monthly variability during this period, we calculated the weighted average  
 19 regression slope among the 28 reflection points, R, using Eq. (3). In Eq. (3), r<sub>i</sub> stands for the  
 20 regression slope for reflection point i, w<sub>i</sub> is the weight which is defined as the reciprocal of the  
 21 square of the one sigma uncertainty of the regression slope, σ<sub>i</sub>.

$$22 \quad R_{\text{monthly}}^{\text{CLARS}} = \frac{\sum_{i=1}^{i=28} r_i w_i}{\sum_{i=1}^{i=28} w_i}, \text{ where } w_i = \frac{1}{\sigma_i^2} \quad (3)$$

23

### 24 3 Results



1 In this section, we describe the monthly and multi-year trends of the basin average regression  
2 slope observed by CLARS-FTS. Figure 2 shows the time series of the Los Angeles basin  
3 weighted average monthly  $X\text{CH}_4(\text{XS})/X\text{CO}_2(\text{XS})$  regression slopes,  $R$ , and their uncertainties  
4 observed by the CLARS-FTS from September 2011 to May 2015. During this period,  $R$  ranged  
5 from 5.4 to 7.7 ppb  $\text{CH}_4$  ( $\text{ppm CO}_2$ )<sup>-1</sup> with an overall mean of 6.5 ppb  $\text{CH}_4$  ( $\text{ppm CO}_2$ )<sup>-1</sup>. This is  
6 consistent with previous atmospheric observations:  $7.8\pm 0.8$  ppb  $\text{ppm}^{-1}$  from TCCON in 2007-  
7 2008,  $6.7\pm 0.6$  ppb  $\text{ppm}^{-1}$  from ARCTAS in 2008, and  $6.7\pm 0.0$  ppb  $\text{ppm}^{-1}$  from CalNex in 2010  
8 (Wunch et al., 2009; Wennberg et al., 2012; Peischl et al., 2013). CLARS-FTS observations  
9 showed significant monthly fluctuations. The monthly variability in the slope was -8% to +5% in  
10 2011, -9% to +22% in 2012, -13% to +11% in 2013, -18% to +11% in 2014 and -8% to +11% in  
11 2015. Monthly variability reported here spans the minimum and maximum deviations from the  
12 annual monthly mean for each year. Monthly variability for 2011 and 2015 was calculated based  
13 on partial annual data (that is, from September to December for 2011 and from January to  
14 August for 2015). In general, we observed peaks in late summer, fall and winter:  $R$  exceeded 7  
15 ppb  $\text{CH}_4$  ( $\text{ppm CO}_2$ )<sup>-1</sup> in August 2012, December 2012, November 2013, August 2014,  
16 September 2014, November 2014 and August 2015. The smallest values of  $R$  were observed in  
17 the spring and early summer. Typically,  $R$  dipped below 6 ppb  $\text{CH}_4$  ( $\text{ppm CO}_2$ )<sup>-1</sup> in May-June,  
18 2012, June 2013, and March 2013.

19 Figure 3 compares the year-to-year monthly values of  $R$  to the four-year mean values. The  
20 weighted four-year mean values showed maxima in August and September, at 7.0 ppb  $\text{CH}_4$  ( $\text{ppm}$   
21  $\text{CO}_2$ )<sup>-1</sup>. Minima occurred in March when the weighted monthly mean was 5.8 ppb  $\text{CH}_4$  ( $\text{ppm}$   
22  $\text{CO}_2$ )<sup>-1</sup>. The fall peak was also observed by TCCON observations in Pasadena from 2007 to 2008  
23 (Wennberg et al., 2012). However, no winter peak was observed in their study. CLARS  
24 observations showed multi-year variability for some months but not others. To better understand  
25 the seasonal year-to-year trends in  $R$ , we plotted the yearly trends for fall (September, October  
26 and November), winter (December, January and February), spring (March, April and May) and  
27 summer (June, July and August) in Fig. 4. A 15% increase in  $R$  over Los Angeles was observed  
28 in the fall season over the last few years.  $R$  increased from 6.2 ppb  $\text{CH}_4$  ( $\text{ppm CO}_2$ )<sup>-1</sup> in 2012 to  
29 7.1 ppb  $\text{CH}_4$  ( $\text{ppm CO}_2$ )<sup>-1</sup> in 2014. This increasing trend was also observed in summer from 2012  
30 to 2014. However, the summer value decreased again from 2014 to 2015. No year-to-year



1 change was observed in spring. In winter, there were some year-to-year changes but no obvious  
 2 increasing or decreasing trend over the study period. The annual average R value showed no  
 3 significant trend and less than 4% year-to-year variability between 2011 and 2015.

4 For comparison, we also calculated the CH<sub>4</sub>:CO<sub>2</sub> emission ratio based on the bottom-up emission  
 5 inventory. California Air Resources Board (CARB) reported statewide total emissions of CH<sub>4</sub>  
 6 and CO<sub>2</sub> through 2013 ([http://www.arb.ca.gov/app/ghg/2000\\_2013/ghg\\_sector.php](http://www.arb.ca.gov/app/ghg/2000_2013/ghg_sector.php)). For CO<sub>2</sub>,  
 7 statewide emissions were 384, 389 and 387 Tg CO<sub>2</sub> per year in 2011, 2012, and 2013  
 8 respectively. Following Wong et al. (2015), we downscaled the statewide CO<sub>2</sub> emissions by  
 9 fractional population (43% of state population) to obtain 165, 167 and 166 Tg CO<sub>2</sub> per year in  
 10 2011, 2012 and 2013, respectively, for emissions from the South Coast Air Basin. For CH<sub>4</sub>,  
 11 bottom-up emissions of 1629, 1636 and 1644 Gg CH<sub>4</sub> per year were reported by CARB in 2011,  
 12 2012 and 2013 respectively. Following the approach used by Wong et al. (2015), we estimated  
 13 the emissions from the South Coast Air Basin by subtracting the agriculture and forestry  
 14 emissions from the total emissions and then apportioning the emissions by population. This gave  
 15 us emissions of 301, 297 and 300 Gg CH<sub>4</sub> per year in the South Coast Air Basin from 2011 to  
 16 2013. The bottom-up estimate of R, the CH<sub>4</sub>/CO<sub>2</sub> emission ratio, was calculated from Eq. (4),  
 17 where  $E_{\text{CH}_4}|_{\text{annual}}^{\text{inventory}}$  is the downscaled CARB annual total CH<sub>4</sub> emissions,  $E_{\text{CO}_2}|_{\text{annual}}^{\text{inventory}}$  is the  
 18 downscaled CARB annual total CO<sub>2</sub> emissions and  $\frac{\text{MW}_{\text{CH}_4}}{\text{MW}_{\text{CO}_2}}$  is the ratio of the molecular weights  
 19 of CH<sub>4</sub> and CO<sub>2</sub> (that is  $\frac{16 \text{ g CH}_4/\text{mole}}{44 \text{ g CO}_2/\text{mole}}$ ).

$$20 \quad R_{\text{annual}}^{\text{inventory}} = \frac{E_{\text{CH}_4}|_{\text{annual}}^{\text{inventory}}}{E_{\text{CO}_2}|_{\text{annual}}^{\text{inventory}}} \times \frac{\text{MW}_{\text{CO}_2}}{\text{MW}_{\text{CH}_4}} \quad (4)$$

21 Using the downscaled CARB emission estimates for the South Coast Air Basin yields annual R  
 22 values of 5.0, 4.9 and 5.0 ppb CH<sub>4</sub> (ppm CO<sub>2</sub>)<sup>-1</sup> for 2011, 2012 and 2013, respectively. Figure 4  
 23 shows that the annual R values determined from CLARS observations are typically in the 6.3 –  
 24 6.7 range. Thus, the inventory-based R value systematically underestimated the observed annual  
 25 R values by ~30%.

26



## 1 **4 Discussion**

2 We can rearrange Eq. (4) to estimate monthly CH<sub>4</sub> emissions from the South Coast Air Basin  
3 using the CH<sub>4</sub>/CO<sub>2</sub> regression slope R determined from CLARS observations and an inventory-  
4 based estimate of monthly CO<sub>2</sub> emissions (Wong et al., 2015).

$$5 \quad E_{\text{CH}_4}^{\text{top-down}}|_{\text{monthly}} = R|_{\text{monthly}}^{\text{CLARS}} \times E_{\text{CO}_2}^{\text{inventory}}|_{\text{monthly}} \times \frac{MW_{\text{CH}_4}}{MW_{\text{CO}_2}} \quad (5)$$

6 However, this requires estimates of the monthly CO<sub>2</sub> emissions from the South Coast Air Basin.

### 7 **4.1 Estimating Monthly CO<sub>2</sub> emissions**

8 This subsection explores the available CO<sub>2</sub> emission database ( $E_{\text{CO}_2}|_{\text{monthly}}$ ) for the basin.  
9 CARB reported annual bottom-up statewide CO<sub>2</sub> emissions from 2011 to 2013. As described in  
10 the results section, we estimated the annual emissions in the South Coast Air Basin by  
11 apportioning the statewide emissions using the ratio of population in the South Coast Air Basin  
12 to the state population. Because there is no monthly statewide emissions information available,  
13 we distributed the annual CO<sub>2</sub> emission evenly over twelve months (shown as solid light blue  
14 line in Fig. 5). Data in 2014 and 2015 (shown as light blue line) are extrapolated using statewide  
15 annual fuel consumption data provided by the Energy Information Administration  
16 (<http://www.eia.gov/dnav/ng/hist/n9140us2M.htm>;  
17 <http://www.eia.gov/dnav/pet/hist/LeafHandler.ashx?n=PET&s=A103450061&f=M>).

18 In addition to the official CARB emission inventory, three CO<sub>2</sub> emission data products provide  
19 monthly temporal resolution for the South Coast Air Basin for our observational period.

20 1. Hestia – The Hestia fossil fuel CO<sub>2</sub> emissions data product provides sectoral bottom-up  
21 emissions at the building and street level on hourly timescales (<http://hestia.project.asu.edu>).  
22 Data are available for the South Coast Air Basin for the years 2011 and 2012. Here, we  
23 calculated the monthly total CO<sub>2</sub> emissions for the South Coast Air Basin domain based on  
24 the Hestia 1.3 km x 1.3 km hourly gridded version 1.0 (shown by the solid black line in Fig.  
25 5). We defined the South Coast Air Basin domain as the rectangular box bounded by 118.83°  
26 W, 116.67° W, 33.38°N and 34.77°N. Because there are no data after 2012, we extrapolated





1 the emissions from 2012 to 2015 (shown as a faded black line in Fig. 5) using the same  
2 approach described above.

3 2. ODIAC – Open-source Data Inventory for Anthropogenic CO<sub>2</sub> (ODIAC) provides global  
4 emission fields of fossil fuel CO<sub>2</sub> emission with 1 km × 1 km spatial sampling on a monthly  
5 basis. ODIAC is based on CO<sub>2</sub> emission estimates from the Carbon Dioxide Information and  
6 Analysis Center (CDIAC), fuel consumption statistics published by British Petroleum,  
7 satellite-observed nightlights and a global power plant database (Oda and Maksyutov, 2011).  
8 The monthly CO<sub>2</sub> emissions for the South Coast Air Basin domain from September 2011 to  
9 December 2014 are shown as the solid red line in Fig. 5. Data in 2015 (shown as the faded  
10 red line) are projected using the same approach used to extrapolate the Hestia emissions.

11 3. FFDAS - Fossil Fuel Data Assimilation System (FFDAS) provides global monthly/hourly  
12 sectoral fossil fuel CO<sub>2</sub> emission with 0.1° × 0.1° (approx. 10 km × 10 km) spatial sampling  
13 (Asefi-Najafabady et al., 2014). This data product is derived from an optimization of the  
14 Kaya identity constrained by national fossil fuel CO<sub>2</sub> emissions from the International  
15 Energy Agency, satellite-observed nightlights, population, and the Ventus power plant  
16 dataset. Emissions are available through 2012 (shown as the solid green line). Data from  
17 2013 and onwards (shown as the faded green line) are extrapolated using the same method  
18 described previously for CARB, Hestia and ODIAC.

19 As shown in Fig. 5, there are differences as large as 3 Tg CO<sub>2</sub> per month among the three  
20 gridded datasets: Hestia, ODIAC and FFDAS. The differences result from 1) emission  
21 calculation methods, 2) the underlying dataset used in the emission calculations and, 3) spatial  
22 modeling. Hestia is derived primarily from local data in the South Coast Air Basin while ODIAC  
23 and FFDAS are based primarily on national and global proxy approaches. It has been shown that  
24 the use of a global dataset may underestimate emissions in Los Angeles by up to 18% (Brioude  
25 et al., 2013). Despite the systematic differences, all three gridded emission datasets show very  
26 similar monthly variability, with peaks in summer and winter. Based on the source  
27 apportionment in Hestia, the summer peak is due to electricity usage (air conditioning) and the  
28 winter peak is due to space heating. In all three datasets, fossil fuel CO<sub>2</sub> emissions in the basin  
29 show -9 to +14% monthly fluctuations about the annual mean.



1 We believe the Hestia data product provide the most accurate CO<sub>2</sub> emission estimates for the  
2 South Coast Air Basin among all available databases. Therefore, we used the Hestia CO<sub>2</sub>  
3 emissions in our calculations to estimate CH<sub>4</sub> emissions.

#### 4 **4.2 Deriving top-down monthly CH<sub>4</sub> emissions**

5 This subsection explains the monthly and annual trends of our methane emission estimates.

6 Figure 6 shows the time series of monthly methane emissions computed from Eq. (5). Shaded  
7 areas represent the 1 $\sigma$  uncertainties of the derived emissions. Uncertainties are propagated from  
8 the uncertainties of CLARS-FTS XCH<sub>4(XS)XCO<sub>2(XS)</sub> regression slopes and CO<sub>2</sub> emissions. For  
9 CO<sub>2</sub> emissions, we assumed a 10% uncertainty in the Hestia monthly CO<sub>2</sub> emissions (K. Gurney,  
10 personal communication, 2016).</sub>

11 Derived methane emission estimates ranged from 23 to 39 Gg CH<sub>4</sub> per month. Methane emission  
12 peaks occurred in late summer/early fall and winter months. Distinct peaks of methane emission  
13 occurred in December 2011, August 2012 and December 2012 when methane emissions  
14 exceeded 33 Gg per month. In 2013 and 2014, the summer and fall peaks were less prominent  
15 than in 2012. Minimum methane emissions occurred in late spring/early summer when emissions  
16 dropped below 27 Gg per month. The monthly variability in methane emissions was -12 to +16%  
17 in 2011, -13% to +31% in 2012, -19% to +14% in 2013, -16% to +17% in 2014 and -14% to  
18 +17% in 2015. Monthly variability reported here is the minimum and maximum percent  
19 difference from the annual average. Note that monthly variability in 2011 and 2015 was  
20 calculated based on partial annual data.

21 Figure 7 plots the monthly patterns of CLARS-FTS inferred methane emissions for each year.  
22 The inferred methane emission estimates showed a bimodal distribution with peaks during the  
23 winter and the late summer/early fall. The weighted monthly average over this period showed  
24 maxima in January, August and December at 31, 33 and 32 Gg CH<sub>4</sub> per month. The weighted  
25 monthly average gradually decreased from January to June when methane emission reached a  
26 minimum of 25 Gg CH<sub>4</sub> per month. No statistically significant interannual seasonal variability  
27 was observed.



### 1 **4.3 Yearly trends in top-down CH<sub>4</sub> emissions**

2 Figure 8 shows the estimated CH<sub>4</sub> annual emissions for the South Coast Air Basin from 2011 to  
3 2015. The annual methane emission derived for the South Coast Air Basin was 345 Gg CH<sub>4</sub> per  
4 year in 2011. Derived emission increased to 356 Gg CH<sub>4</sub> per year in 2013. Since then, there has  
5 been a decreasing trend reaching 325 Gg CH<sub>4</sub> per year in 2015. Due to the large uncertainty  
6 propagated mainly from CO<sub>2</sub> emissions, we derived a decreasing trend of  $-5 \pm 4$  Gg CH<sub>4</sub> per year  
7 with only 25% confidence level.

8 Figure 9 compares all reported CH<sub>4</sub> annual total emission estimates for the South Coast Air  
9 Basin in the past ten years. These estimates were derived based on in situ ground observations  
10 (Hsu et al., 2010), column measurements (Wunch et al., 2009, Wennberg et al., 2012; Wong et  
11 al., 2015) and aircraft measurements (Peischl et al., 2013; Wennberg et al., 2012; Wecht et al.,  
12 2014; Cui et al., 2015) in the Los Angeles basin. Among all the previous studies, only one study  
13 (Wong et al., 2015) estimated methane emissions for the period between 2011 and 2015. Our  
14 estimates for 2011 to 2013 were lower but within uncertainties with the estimates reported by  
15 Wong et al. (2015). The difference in the estimated methane emissions between the present study  
16 and Wong et al. (2015) is due to differences in the CO<sub>2</sub> reference emissions used in the  
17 calculations. Hestia CO<sub>2</sub> emissions used in the present calculations were lower than the  
18 population-scaled CARB emissions used in Wong et al., 2015. The rest of the studies were based  
19 on methane observations from 2007 to 2010. Despite the different study periods, methane  
20 emission estimates from our study are inconsistent with previous top-down estimates. About half  
21 of previously reported methane emission estimates were focused on the CALNEX field  
22 experiment in May and June 2010. The annual methane emission estimates from these studies  
23 could be underestimated as we observed that methane emissions tend to be lowest during these  
24 months. Comparing our results to the bottom-up inventory, the scaled CARB CH<sub>4</sub> emissions  
25 from 2011 to 2013 were 2-31% lower than our estimates.

### 26 **4.4 Analysis assumptions**

27 In this subsection, we discuss the analysis assumptions used to derive CH<sub>4</sub> emissions for the  
28 South Coast Air Basin using CLARS-FTS observations.



- 1 • **Spatial and temporal representation based on CLARS-FTS measurement technique.**  
2 We assumed that the CLARS-FTS measurement domain is representative of the South Coast  
3 Air Basin. The CLARS-FTS measurement domain covers 67% of CO<sub>2</sub> emissions in the  
4 South Coast Air Basin spatial domain according to the Hestia CO<sub>2</sub> data product. Therefore,  
5 the CLARS-FTS observations are more representative of the sampled area in the South Coast  
6 Air Basin than the entire basin. In addition, our methane emission estimates were based on  
7 daytime-only observations.
- 8 • **Spatial and temporal bias due to data filtering.** CLARS-FTS samples the Los Angeles  
9 basin using its standard measurement sequence. However, as described in Wong et al.  
10 (2015), certain months of the year are more prone to cloud and aerosol interference in the  
11 Los Angeles basin. This may introduce biases in the monthly sampling of post-filtered data.  
12 To accurately estimate the LA basin value, we used the weighted average  $XCH_{4(XS)}/XCO_{2(XS)}$   
13 regression slope, as the statistical weight for each reflection point is based on the number of  
14 samples passing through the data quality filters. We also performed a bootstrap analysis to  
15 ensure that there is no sampling bias in the regression slopes (Efron and Tibshirani, 1993).
- 16 • **Seasonal bias due to transport variability.** Changes in meteorology patterns in summer vs.  
17 winter can lead to a seasonal dependence on the observations' footprint, which is the  
18 sensitivity of the observations to changes in emissions. In the Los Angeles basin, the  
19 prevailing winds are typically northwesterly and onshore throughout the year, except for  
20 Santa Ana events (Conil and Hall, 2006). During Santa Ana events, which typically occur  
21 during the period from October to March, the wind patterns in the basin shift to easterly and  
22 offshore flow (Hughes and Hall, 2010). We investigated the impact of Santa Ana events on  
23 our results using the Santa Ana Index to remove observations during Santa Ana events  
24 (Hughes and Hall, 2010; Conil and Hall, 2006; <http://meteora.ucsd.edu/weather/>). A  
25 correlation analysis showed that applying the Santa Ana Index filter did not cause any  
26 statistically significant bias on the CLARS monthly CH<sub>4</sub>:CO<sub>2</sub> ratios. This insensitivity is  
27 likely due to the effect of spatial averaging over 28 slant column measurements that span a  
28 50 x 100 km<sup>2</sup> spatial domain in the Los Angeles basin, mitigating the effect of transport  
29 variability, especially when compared with measurements from individual tower sites. A  
30 more diagnostic approach involving the application of a high-resolution tracer transport



1 model to investigate potential transport-induced biases on CLARS-FTS results will be  
2 carried out in the future.

### 3 **4.5 Exploring seasonal variability from major CH<sub>4</sub> emission sources**

4 Currently, no monthly methane emission database is publicly available for comparison with our  
5 top-down estimates during our observational period. In this subsection of the paper, we review  
6 previous studies of the seasonal emissions variability from major methane sources (landfills,  
7 dairies, wastewater treatment plants and natural gas system leakage) to understand possible  
8 contributions to the observed monthly variability in total CH<sub>4</sub> emission in the South Coast Air  
9 Basin.

- 10 • **Landfills.** Landfills are major emitters of CH<sub>4</sub> in the basin. Previous studies suggested that  
11 landfills could contribute 41-63% of total annual methane emissions (Peischl et al., 2013;  
12 Wennberg et al., 2012; Hsu et al., 2010). The seasonal variability in landfill CH<sub>4</sub> emissions is  
13 poorly understood, however. Peischl et al. (2013) estimated the emissions from two of the  
14 largest landfills in the basin – Olinda Alpha landfill and Puente Hills landfill – based on  
15 aircraft measurements in May and June 2010. Based on observations taken from four flights  
16 in May and one flight in June, their studies found that CH<sub>4</sub> emissions from Olinda Alpha  
17 landfill was almost double in June relative to May while Puente Hills landfill (which was  
18 closed in 2012) showed less than 15% changes in monthly emissions in 2010. Using a  
19 landfill model, Spokas et al. (2015) found that the statewide landfill emissions were largest in  
20 October and smallest in April in 2010. Other observational studies found that CH<sub>4</sub> emissions  
21 from landfills peak in July and August (Shan et al., 2013; Spokas et al., 2011; Tratt et al.,  
22 2014; Goldsmith et al., 2012). These studies suggest that landfills can contribute to the late  
23 summer/early fall peak in the total CH<sub>4</sub> emissions observed by CLARS-FTS but are unlikely  
24 to explain the winter peaks.
- 25 • **Dairies.** Previous observations suggested that dairy farms could contribute 32 – 76 Gg CH<sub>4</sub>  
26 per year in the South Coast Air Basin (Peischl et al., 2013; Wennberg et al., 2012). This  
27 corresponds to 8% to 36% of the reported total annual CH<sub>4</sub> emissions in the studies. In  
28 general, studies on dairies focus on mitigation strategies rather than quantifying temporal  
29 changes in emissions. Limited studies of dairy emissions report peaks in CH<sub>4</sub> emissions in



1 summer and early fall (from June to September), and steady minima in spring and winter  
2 (VanderZaag et al., 2014; VanderZaag et al., 2013; VanderZaag et al., 2010; VanderZaag et  
3 al., 2009; Ulyatt et al., 2002; Kaharabata et al., 1998). These findings imply that dairies can  
4 also be contributing to the summer/early fall peaks in the CLARS-FTS inferred CH<sub>4</sub>  
5 emissions.

- 6 • **Wastewater treatment.** This sector is shown to be responsible for 33% of Los Angeles  
7 County and 9.4% of the South Coast Air Basin (Hsu et al., 2010; Wennberg et al., 2012).  
8 Daelman et al. (2012; 2013) measured CH<sub>4</sub> emissions from a wastewater treatment facility  
9 for one year (2010-2011) and reported up to 40% monthly fluctuations from the mean, with a  
10 maximum in June.
- 11 • **Fossil fuel sources.** Recent studies based on mobile, stationary and airborne measurements  
12 of methane in Los Angeles indicated that fossil fuel sources contribute 47% to 90% of the  
13 total CH<sub>4</sub> emissions in the basin (Wennberg et al., 2012; Townsend-Small et al. 2012; Peischl  
14 et al., 2013; Hopkins et al., 2015). Wennberg et al. (2012) and Peischl et al. (2013) suggested  
15 that fugitive emission from natural gas distribution system leakage contributes to the gaps  
16 between bottom-up and top-down total CH<sub>4</sub> emissions in the South Coast Air Basin. McKain  
17 et al. (2014) found little seasonal dependence (<10%) on the emissions from the natural gas  
18 system in Boston, Massachusetts. Their studies showed a leakage rate of  $2.7 \pm 0.6\%$  from the  
19 natural gas system. Wennberg et al. (2012) reported a consistent leakage rate from the natural  
20 gas system in Los Angeles and suggested that most of the leakages from such systems are  
21 likely to occur in residential/commercial areas where the distribution system ends. Publicly  
22 available natural gas consumption data from residential and commercial sectors in the South  
23 Coast Air Basin show a significant seasonal cycle with a maximum in winter due to heating  
24 (<https://energydatarequest.socalgas.com/>). Wennberg et al. (2012) and McKain et al. (2014)  
25 observed that the leakage rate from the natural gas system is constant throughout the year and  
26 suggested that the majority of leakage occurs in the distribution system to the residential and  
27 commercial sectors. This conclusion is reasonable since the natural gas distribution pipeline  
28 system is pressure-regulated at several points, and leakage should be independent of  
29 consumption to first order. However, this is not the case for natural gas storage facilities  
30 which are pressurized to higher levels in the summer and late fall in Southern California to  
31 respond to increased demands for summertime electric power generation for air conditioning



1 and wintertime space heating. In October, 2015, a massive leak began at an underground well  
2 pipe at the Aliso Canyon (Los Angeles) natural gas storage facility as it was being  
3 pressurized to provide wintertime reserves. While this leak was unprecedented in scale, it  
4 raises the question whether smaller fugitive leaks in the storage infrastructure from this and  
5 numerous other above- and below-ground reservoirs contribute to the seasonal variability  
6 observed in CLARS-FTS data. The Aliso Canyon leak resulted in very large increases (as  
7 much as a factor of 10) in the observed instantaneous values of  $XCH_{4(XS)}/XCO_{2(XS)}$  throughout  
8 the entire CLARS-FTS field of regard (Wong et al., in prep.). Since CLARS-FTS is capable  
9 of resolving  $CH_4$  enhancements that are significantly smaller than those caused by the Aliso  
10 Canyon leak, perhaps seasonally-varying fugitive emissions from natural gas storage  
11 facilities and associated infrastructure are partially responsible for the observed monthly  
12 variability. Enhanced long-term monitoring for fugitive emissions will be required to test this  
13 hypothesis.

14

## 15 **5 Summary and Conclusions**

16 Using CLARS-FTS mountaintop remote sensing observations from Mount Wilson along with  
17 tracer-tracer  $CH_4:CO_2$  correlation analyses, we estimated the monthly variability in  $CH_4:CO_2$  and  
18 top-down  $CH_4$  emissions from the South Coast Air Basin from 2011-2015. Significant monthly  
19 variability (-18% to +22%) in  $CH_4:CO_2$  was observed. Double peaks in late summer/early fall  
20 and winter occurred consistently during the study period. The fall peak in the  $CH_4:CO_2$  ratios  
21 was also observed by TCCON (Wennberg et al., 2012). The CLARS-FTS  $XCH_{4(XS)}/XCO_{2(XS)}$   
22 regression slopes showed -7% to 10% year-to-year seasonal variability, with an increasing trend  
23 in the fall season from 2012 to 2014. The annual average  $XCH_{4(XS)}/XCO_{2(XS)}$  regression slopes  
24 showed less than 4% year-to-year variability between 2011 and 2015.

25 Using the best available estimates of  $CO_2$  emissions, top-down estimates of  $CH_4$  emissions were  
26 determined using the emission ratio method. Repeatable peaks in late summer/early fall and  
27 winter were observed between 2011 and 2015. There were significant monthly fluctuations (-  
28 19% to +31% from annual mean and a maximum month-to-month change of 47%) in the  
29 inferred methane emissions in the basin. Based on previous studies on the seasonal variability of



1 CH<sub>4</sub> emissions from CH<sub>4</sub> sources, we concluded that landfills, dairies and wastewater treatment  
2 facilities are likely sources of the peak CH<sub>4</sub> emissions in late summer/early fall. Fugitive  
3 emissions from natural gas storage facilities and associated infrastructure may contribute to both  
4 the late summer and late fall peaks.

5 No significant trend in CH<sub>4</sub> emissions ( $-5 \pm 4$  Gg CH<sub>4</sub> per year with a 25% confidence level due  
6 to the uncertainty in CO<sub>2</sub> emissions) could be discerned over the 2011 to 2015 time period. The  
7 population-scaled bottom-up CH<sub>4</sub> emissions from 2011 to 2013 were 2-31% lower than our top-  
8 down estimates. These results are consistent with previous studies (Wunch et al., 2009; Hsu et  
9 al., 2010; Wennberg et al., 2012; Peischl et al., 2013; Wong et al., 2015). A combination of  
10 several measurement and modeling strategies are necessary to further disentangle the monthly  
11 variability of methane sources in the Los Angeles basin.

12

### 13 **Acknowledgements**

14 The research in this study was performed at the Jet Propulsion Laboratory, California Institute of  
15 Technology, under a contract with the National Aeronautics and Space Administration. KWW  
16 thanks the California Air Resources Board, NIST GHG and Climate Science Program, and the  
17 W.M. Keck Institute for Space Studies for support. The authors would like to acknowledge our  
18 colleagues at JPL and California Institute of Technology, and Risa Patarasuk at Arizona State  
19 University for helpful comments and suggestions.

20





## 1 **References**

2

3 Asefi-Najafabady, S., Rayner, P. J., Gurney, K. R., McRobert, A., Song, Y., Coltin, K., Huang,  
4 J., Elvidge, C., and Baugh, K.: A multiyear, global gridded fossil fuel CO<sub>2</sub> emission data  
5 product: Evaluation and analysis of results, *J. Geophys. Res.-Atmos.*, 118, 1–19,  
6 doi:10.1002/2013JD021296, 2014.

7 Brioude, J., Angevine, W. M., Ahmadov, R., Kim, S.-W., Evan, S., McKeen, S., Hsie, E.-Y.,  
8 Frost, G. J., Neuman, J. A., Pollack, I. B., Peischl, J., Ryerson, T. B., Holloway, J., Brown, S. S.,  
9 Nowak, J. B., Roberts, J. M., Wofsy, S. C., Santoni, G. W., Oda, T., and Trainer, M.: Top-down  
10 estimate of surface flux in the Los Angeles Basin using a mesoscale inverse modeling technique:  
11 Assessing anthropogenic emissions of CO, NO<sub>x</sub> and CO<sub>2</sub> and their impacts, *Atmos. Chem.*  
12 *Phys.*, 13, 3661–3677, 2013.

13 California Air Resources Board: Greenhouse gas emission inventory – Query tool for years 2000  
14 to 2013, 8th Edn., [http://www.arb.ca.gov/app/ghg/2000\\_2013/ghg\\_sector.php](http://www.arb.ca.gov/app/ghg/2000_2013/ghg_sector.php), (last access:  
15 January 2015), 2013.

16 Conil, S., and Hall, A.: Local regimes of Atmospheric Variability: A case study of Southern  
17 California, *J. Clim.*, 19, 4308, 2006.

18 Cui, Y. Y., Brioude, J., McKeen, S. A., Angevine, W. M., Kim, S.-W., Frost, G. J., Ahmadov,  
19 R., Peischl, J., Bousserrez, N., Liu, Z., Ryerson, T. B., Wofsy, S. C., Santoni, G. W., Kort, E. A.,  
20 Fischer, M. L., and Trainer, M.: Top-down estimate of methane emissions in California using a  
21 mesoscale inverse modeling technique: The South Coast Air Basin, *J. Geophys. Res.-Atmos.*,  
22 120, 6698–6711, 2015.

23 Daelman, M. R., van Voorthuizen, E. M., van Dongen, U. G., Volcke, E. I., and van Loosdrecht,  
24 M. C.: Methane emission during municipal wastewater treatment, *Water Res.*, 46, 3657–3670,  
25 2012.



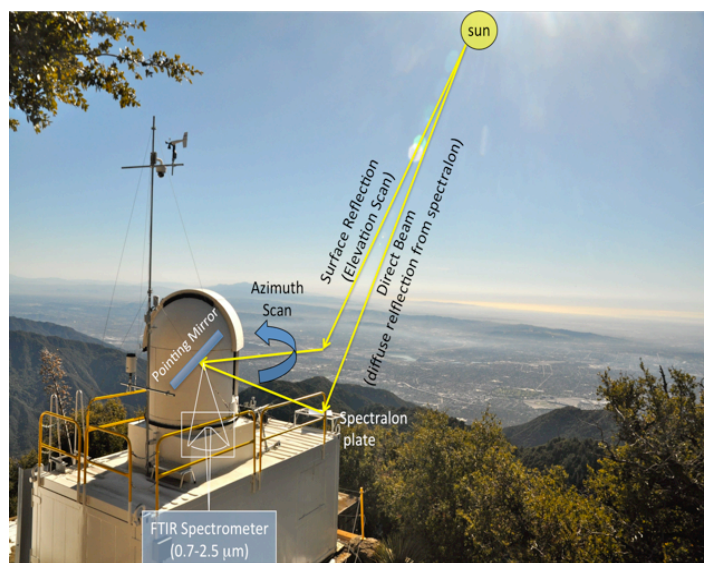
- 1 Daelman, M. R., van Voorthuizen, E. M., van Dongen, L. G., Volcke, E. I., and van Loosdrecht,  
2 M. C.: Methane and nitrous oxide emissions from municipal wastewater treatment - results from  
3 a long-term study, *Water Sci. Technol.*, 67, 2350–5, 2013.
- 4 Efron, B. and Tibshirani, R.: *An Introduction to the Bootstrap*, Vol. 57, CRC press, Boca Raton,  
5 Florida, USA, 45–82, 1993.
- 6 Gao, Z., Yuan, H., Ma, W., Li, J., Liu, X., and Desjardins, R. L.: Diurnal and seasonal patterns of  
7 methane emissions from a dairy operation in North China Plain, *Adv. in Meteorol.*, 1–7, 2011.
- 8 Goldsmith, C. D., Chanton J., Abichou T., Swan, N., Green, R., and Haters, G.: Methane  
9 emissions from 20 landfills across the United States using vertical radial plume mapping, *Air  
10 Waste Manage.*, 62 (2), 183–197, 2012.
- 11 Hopkins, F. M., Kort, E. A., Bush, S. E., Ehleringer, J. R., Lai, C.-T., Blake, D. R., and  
12 Randerson, J. T.: Spatial patterns and source attribution of urban methane in the Los Angeles  
13 Basin, *JGR-A* accepted.
- 14 Hsu, Y.-K., VanCuren, T., Park, S., Jakober, C., Herner, J., FitzGibbon, M., Blake, D., and  
15 Parrish, D. D.: Methane emissions inventory verification in southern California. *Atmos.  
16 Environ.*, 44, 1–7, 2009.
- 17 Hughes, M., and Hall, A.: Local and synoptic mechanisms causing Southern California's Santa  
18 Ana winds, *Clim. Dyn.*, 34, 847-857, 2010.
- 19 Jeong, S., Hsu, Y.-K., Andrews, A. E., Bianco, L., Vaca, P., Wilczak, J. M., and Fischer, M. L.:  
20 A multitower measurement network estimate of California's methane emissions. *J. Geophys.  
21 Res.-Atmos.*, 118, 11339–11351, 2013.
- 22 Kaharabata, S. K., Schuepp, P. H., and Desjardins, R. L.: Methane emissions from above ground  
23 open manure slurry tanks. *Global Biogeochem. Cy.*, 12, 545, 1998.



- 1 Mckain, K., Down, A., Raciti, S. M., Budney, J., Hutyra, L. R., and Floerchinger, C.: Methane  
2 emissions from natural gas infrastructure and use in the urban region of Boston, Massachusetts,  
3 P. Natl. Acad. Sci., 112, 1941–1946, 2014.
- 4 Oda, T., and Maksyutov, S.: A very high-resolution (1 km x 1 km) global fossil fuel CO<sub>2</sub>  
5 emission inventory derived using a point source database and satellite observations of nighttime  
6 lights, Atmos. Chem. Phys., 11, 543–556, 2011.
- 7 Spokas, K., Bogner, J., and Chanton, J.: A process-based inventory model for landfill CH<sub>4</sub>  
8 emissions inclusive of seasonal soil microclimate and CH<sub>4</sub> oxidation, J. Geophys. Res., 116,  
9 G04017, 2011.
- 10 Shan, J., Iacoboni, M., and Ferrante, R.: Estimating greenhouse gas emissions from three  
11 Southern California landfill sites, Proceedings of SWANA's 2013 Landfill Gas Symposium,  
12 Silver Springs, MD, 2013.
- 13 Tratt, D. M., Buckland, K. N., Hall, J. L., Johnson, P. D., Keim, E. R., Leifer, I., Westberg, K.,  
14 and Young, S. J.: Airborne visualization and quantification of discrete methane sources in the  
15 environment, Remote Sens. Environ., 154, 74–88, 2014.
- 16 Ulyatt, M. J., Lassey, K. R., Shelton, I. D., and Walker, C. F.: Seasonal variation in methane  
17 emission from dairy cows and breeding ewes grazing ryegrass/white clover pasture in New  
18 Zealand, New Zeal. J. Agr. Res., 45, 227–234, 2002.
- 19 VanderZaag, A. C., Gordon, R. J., Jamieson, R. C., Burton, D. L., and Stratton, G. W.: Gas  
20 emissions from straw covered liquid dairy manure during summer storage and autumn agitation,  
21 Trans. Am. Soc. Agric. Eng., 52, 599–608, 2009.
- 22 VanderZaag, A. C., Gordon, R. J., Jamieson, R. C., Burton, D. L., and Stratton, G. W.: Effects of  
23 winter storage conditions and subsequent agitation on gaseous emissions from liquid dairy  
24 manure, Can. J. Soil. Sci., 90, 229–239, 2010.



- 1 VanderZaag, A. C., Flesch, T. K., Desjardins, R. L., Baldé, H., and Wright, T.: Measuring  
2 methane emissions from two dairy farms: Seasonal and manure-management effects, *Agr. Forest*  
3 *Meteorol.*, 194, 259–267, 2014.
- 4 VanderZaag, A. C., MacDonald, J. D., Evans, L., Vergé, X. P., and Desjardins, R. L.: Towards  
5 an inventory of methane emissions from manure management that is responsive to changes on  
6 Canadian farms, *Environ. Res. Lett.*, 8, 035008, 2013.
- 7 Wecht, K. J., Jacob, D. J., Sulprizio, M. P., Santoni, G. W., Wofsy, S. C., Parker, R., Bosch, H.,  
8 and Worden, J.: Spatially resolving methane emissions in California: constraints from the  
9 CalNex aircraft campaign and from present (GOSAT, TES) and future (TROPOMI,  
10 geostationary) satellite observations, *Atmos. Chem., Phys.*, 14, 8173–8184, 2014.
- 11 Wunch, D., Wennberg, P. O., Toon, G. C., Keppel-Aleks, G., and Yavin, Y. G.: Emissions of  
12 greenhouse gases from a North American megacity, *Geophys. Res. Lett.*, 36, 1–5, 2009.
- 13 Wennberg, P. O., Mui, W., Wunch, D., Kort, E. A., Blake, D. R., Atlas, E. L., Santoni, G. W.,  
14 Wofsy, S. C., Diskin, G. S., Jeong, S., and Fischer, M. L.: On the sources of methane to the Los  
15 Angeles atmosphere, *Environ. Sci. Tech.*, 46, 9282–9289, 2012.
- 16 Wong, K. W., Fu, D., Pongetti, T. J., Newman, S., Kort, E. A., Duren, R., Hsu, Y.-K., Miller, C.  
17 E., Yung, Y. L., and Sander, S. P., Mapping CH<sub>4</sub>: CO<sub>2</sub> ratios in Los Angeles with CLARS-FTS  
18 from Mount Wilson, California, *Atmos. Chem. Phys.*, 15, 241–252, 2015.



1

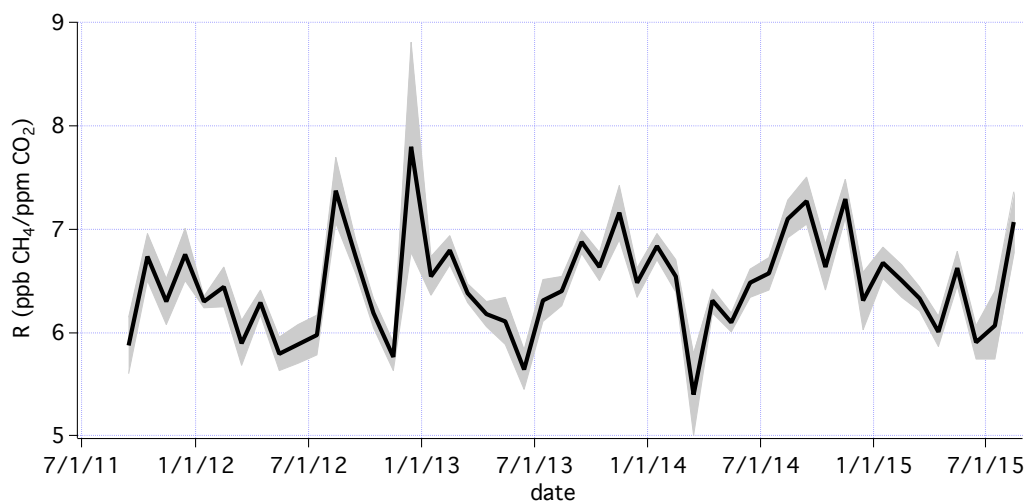


2

3

4 Figure 1. Top: CLARS facility located at 1.67 km above sea level on Mount Wilson, looking  
5 over the Los Angeles basin. Optical paths from direct sun beam and basin surface reflection are  
6 shown as yellow lines. Bottom: Location of 29 reflection points on Mount Wilson (white square)  
7 and in the basin (yellow triangles).

8

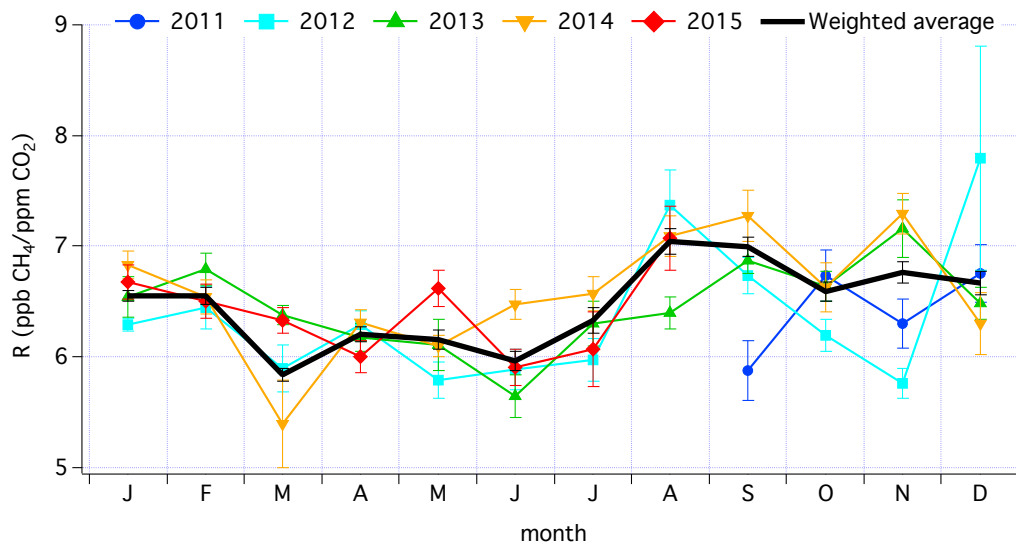


1

2

3 Figure 2. Time series of the Los Angeles basin weighted-average monthly regression slopes of  
4  $XCH_{4(XS)} - XCO_{2(XS)}$  (in unit of  $ppb\ ppm^{-1}$ ) and their uncertainties observed by the CLARS-FTS  
5 in the basin from September 2011 to May 2015. Uncertainties are  $\pm 1\sigma$  of the regression slopes.

6

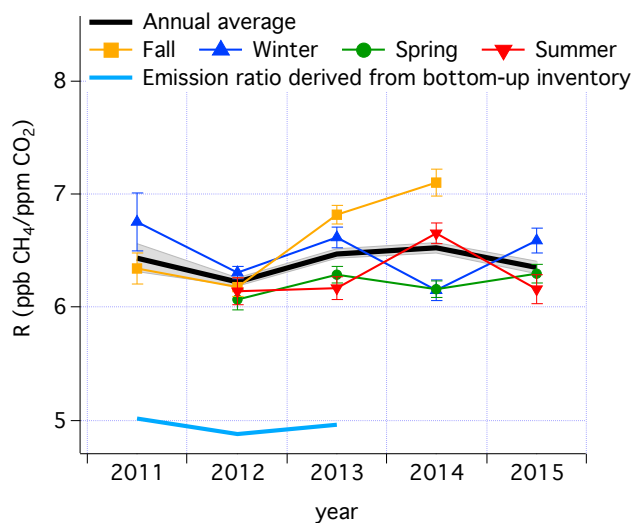


1

2

3 Figure 3. Monthly patterns of the Los Angeles basin weighted-average regression slopes of  
4  $XCH_{4(XS)} - XCO_{2(XS)}$  (in unit of  $ppb\ ppm^{-1}$ ) and their uncertainties observed by the CLARS-FTS  
5 in the basin. Monthly trends are color coded as follows: 2011 in blue, 2012 in cyan, 2013 in  
6 green, 2014 in orange and 2015 in red. Monthly average ratio and its standard deviation over the  
7 entire observational period are shown in black.

8



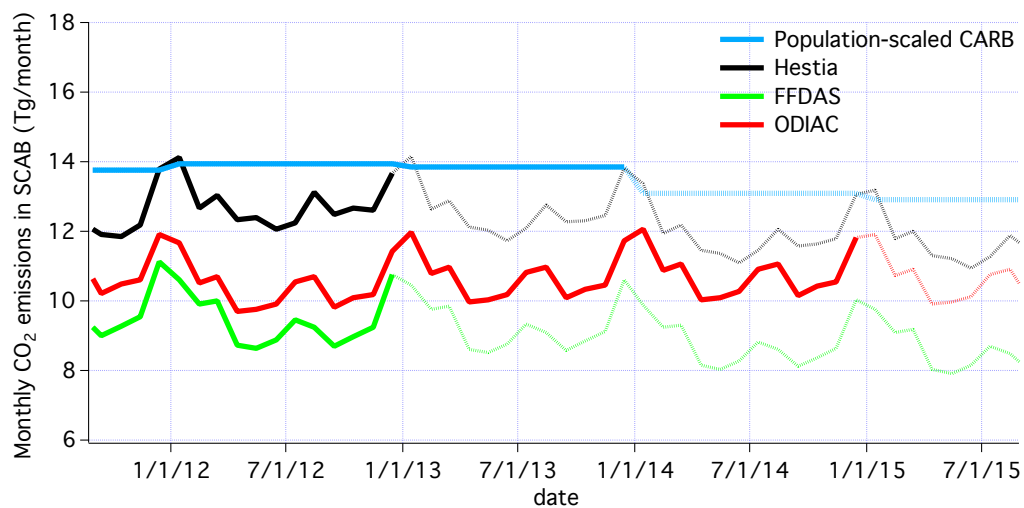
1

2

3 Figure 4. Interannual variability of  $R$  (in units of  $\text{ppb CH}_4 (\text{ppm CO}_2)^{-1}$ ) in fall (orange), winter  
4 (blue), spring (green) and summer (red) from 2011 to 2015. The annual average ratio is shown in  
5 black. Also shown are the  $\pm 1\sigma$  uncertainties. Note that data for 2011 and 2015 are derived from  
6 partial annual observations (that is, September to December for 2011 and January to August for  
7 2015). The  $\text{CH}_4:\text{CO}_2$  ratio based on the population-scaled bottom-up emission inventory from the  
8 California Resources Board is shown in light blue (California Air Resources Board, 2013).

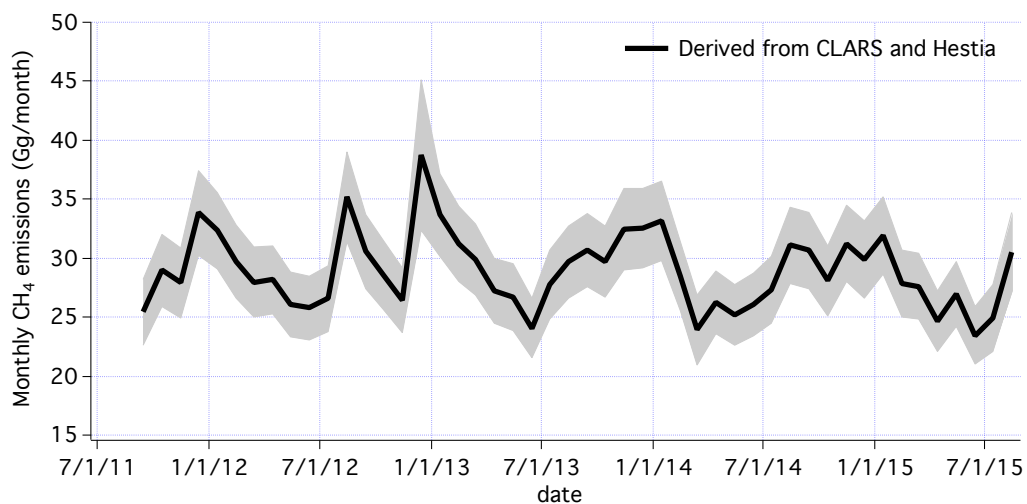
9





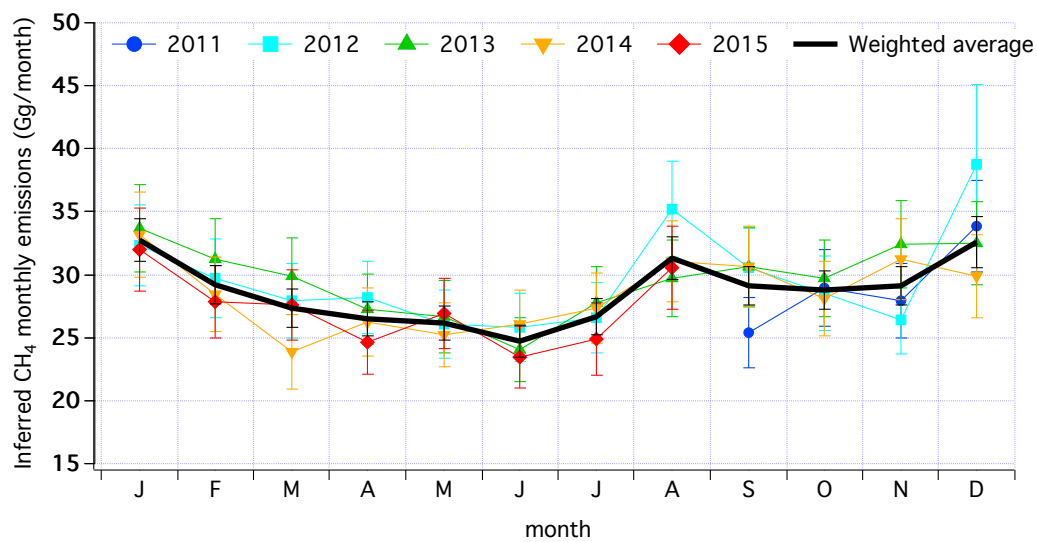
1  
2  
3  
4  
5  
6  
7

Figure 5. Time series of the different CO<sub>2</sub> monthly emissions (in units of Tg per month) from the South Coast Air Basin. Emissions are color coded as follows: Population-scaled CARB in light blue, Hestia in solid black, ODIAC in solid red and FFDAS in solid green. Extrapolated emissions using annual fuel consumption data are shown in faded solid lines.



1  
2  
3  
4  
5  
6  
7

Figure 6. Time series of CLARS-FTS inferred monthly CH<sub>4</sub> emissions (in units of Gg per month) and their 1 $\sigma$  uncertainties from the Los Angeles basin from September 2011 to August 2015. Overall uncertainties are propagated from the uncertainties of CLARS-FTS XCH<sub>4(XS)</sub>—XCO<sub>2(XS)</sub> regression slopes and CO<sub>2</sub> emissions.

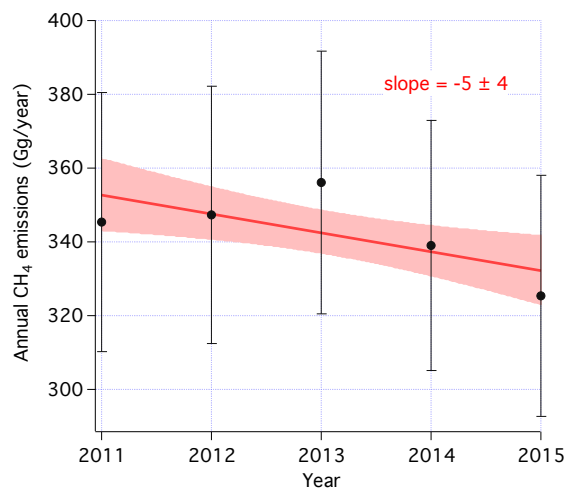


1

2

3 Figure 7. Monthly patterns of derived CH<sub>4</sub> emissions (in units of Gg per month). Error bars  
4 represent the  $\pm 1\sigma$  uncertainties. Derived CH<sub>4</sub> emissions are color coded as follows: 2011 in blue,  
5 2012 in cyan, 2013 in green, 2014 in orange and 2015 in red. Average monthly emissions and  
6 their standard deviations over the entire observational period are shown in black.

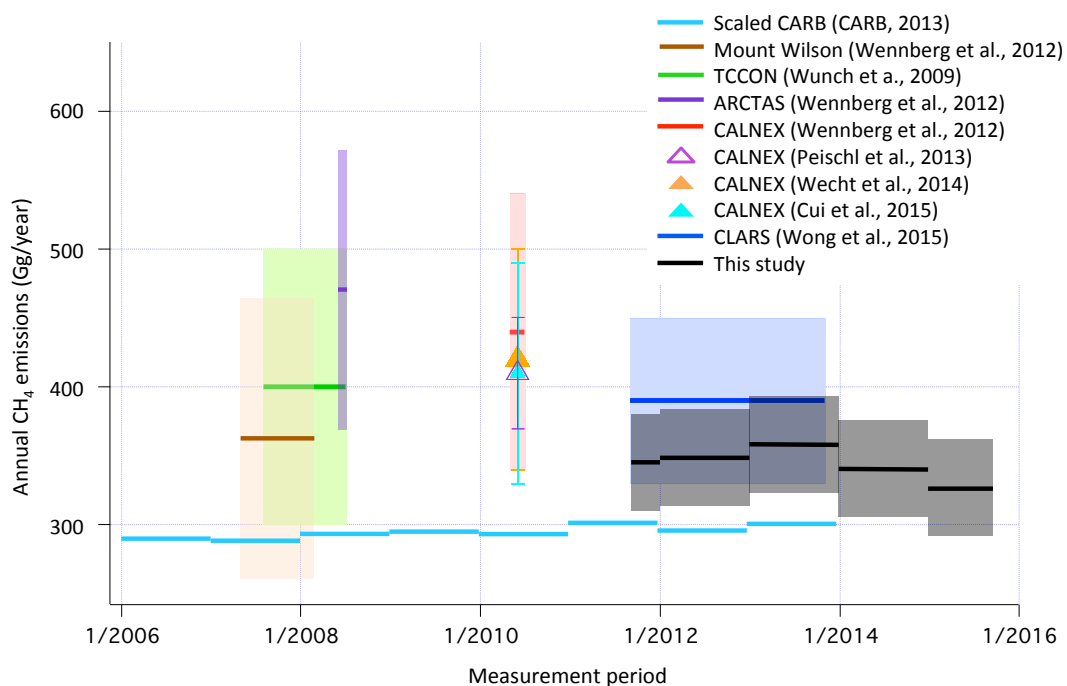
7



1  
2

3 Figure 8. CLARS-FTS inferred annual CH<sub>4</sub> emission estimates (in units of Gg per month), based  
4 on Hestia CO<sub>2</sub> emissions. Red line indicates the regression slope and the shaded area is the 25%  
5 confidence interval.

6



1  
2 Figure 9. Comparison of annual CH<sub>4</sub> emission estimates (in unit of Gg per month) reported in the  
3 past ten years. The Mount Wilson estimate reported by Wennberg et al. (2012) was derived for  
4 the South Coast Air Basin using the emission estimates based on Hsu et al., 2012.